PAPER Nr. : 8

STUDY OF THE UNSTEADY TRANSONIC FLOW ON ROTOR BLADE WITH DIFFERENT TIP SHAPES

BY

A. DESOPPER

ONERA
92320 Châtillon, FRANCE

TENTH EUROPEAN ROTORCRAFT FORUM

AUGUST 28 – 31, 1984 – THE HAGUE, THE NETHERLANDS

STUDY OF THE UNSTEADY TRANSONIC FLOW ON ROTOR BLADE WITH DIFFERENT TIP SHAPES

A. DESOPPER
ONERA
92320 Châtillon, FRANCE

SUMMARY

An unsteady transonic small perturbations method is used to characterize the flow on an helicopter blade in the advancing blade side where unsteady transonic flows occur. Non lifting and lifting unsteady calculation results are presented for different tip shapes.

Non lifting calculation results show the influence of sweep (backward and forward), progressive sweep with taper and anhedral effect on the intensity of the transonic flows.

The lifting calculations concern high advance ratio configurations ($\mu > 0.3$). They are performed on an isolated blade with an angle of attack prescribed along the blade for each azimuthal location. Three blade tips are considered : a rectangular blade and two swept tips. For the three tips the resulting computations compare well with experimental results obtained on a model rotor equiped with absolute pressure tranducers. Experimental and calculated results indicate clearly that the improvement of the performances obtained with the model rotor equiped with the swept tips compared to the ones of the same rotor equiped with rectangular blades, is mainly due to the decrease of the transonic flow intensity observed on the swept tips.

All the results obtained are very encouraging and give a certain confidence in the use of such a method as an help to design efficient tip shapes for fast forward flight.

LIST OF SYMBOLS

$\varepsilon = \frac{1}{AR} = \frac{C}{R}$ = 1/(aspect ratio)

c = chord

Cp_* = pressure coefficient

Cp^* = critical pressure coefficient

Ct = thrust coefficient Cq = power coefficient

M = Mach number

$M\omega r = \frac{\omega R}{a_\infty}$ = tip Mach number

R = blade radius

r = radial station

t = $\Psi - 90°$ = time

Vo = forward velocity

α = total angle of attack
α_1 = angle of attack due to shaft tilting
α_2 = angle of attack due to flapping
α_3 = angle of attack due to induced velocity
δ = thickness ratio
θ_c = collective pitch angle
θ_w = twist angle
$\mu = \frac{V_o}{\omega R}$ = advance ratio
σ = solidity
ϕ = velocity potential
ψ = azimuthal angle
ω = angular speed

1 - INTRODUCTION -

A full calculation of the flow on an helicopter blade would require a three-dimensional unsteady method able of computing various flow conditions, like :

- transonic flows for the advancing blade side,
- flows with large viscous effects for the dynamic stall problem on the retreating blade side,
- development and influence of a very complicated wake system generated by the blades.

Up to now, no practical method exists for such difficult conditions and the studies are generally limited to one aspect of this problem.

At the Aerodynamic Department of ONERA, experimental and theoretical studies of the unsteady transonic flows on the advancing blade side have been performed for about ten years now. The main purpose of these studies is to define some blade tip shapes which improve the aerodynamic and acoustic performances of a rotor by reducing the wave drag and the intensity of the transonic flows that appear on a rectangular blade for fast forward flight speed.

An unsteady transonic small perturbation method is used to compute the unsteady transonic flow of the advancing blade side. Non-lifting and lifting unsteady calculations are presented for different tip shapes.

The non-lifting calculation results show the influence of sweep (backward and forward), progressive sweep with taper and anhedral effect on the intensity of the transonic flows.

The lifting calculations are performed on an isolated blade with an angle of attack prescribed along the blade for each azimuthal location. These calculations concern high advance ratio configurations ($\mu > 0.3$) and three blade tip shapes are considered : a rectangular blade and two progressive swept tips. The results are compared with experimental ones obtained on a model rotor equiped with absolute pressure transducers.

The intent of this paper is to show some interesting features of the unsteady transonic flows that occur in the advancing blade side for fast forward flight speed.

2 - UNSTEADY TRANSONIC SMALL DISTURBANCES METHOD USED FOR THE CALCULATIONS -

2.1 - Non-lifting calculation -

ONERA and US Army RTL at Ames have worked jointly within the framework of an M.O.U. on helicopter aeroelasticity to develop a computer program to solve the low frequency transonic small disturbance equation for rotor blades of nearly arbitrary planform [1-2] .

This equation has the form :

$$(1) \qquad A\frac{\partial^2\phi}{\partial t\,\partial x} = \frac{\partial}{\partial x}\left[B\frac{\partial\phi}{\partial x} + B'\left(\frac{\partial\phi}{\partial x}\right)^2\right] + C\frac{\partial^2\phi}{\partial x\,\partial y} + D\frac{\partial^2\phi}{\partial y^2} + E\frac{\partial^2\phi}{\partial z^2}$$

with

$$A = 2\,M_{\omega R}^2\,\frac{\varepsilon}{\delta^{2/3}}\,(y+\mu\cos t)$$

$$B = \frac{1-M_{\omega R}^2\,(y+\mu\cos t)^2}{\delta^{2/3}}$$

$$C = 2\,M_{\omega R}^2\,\frac{\varepsilon}{\delta^{2/3}}\,\mu\sin t\,(y+\mu\cos t)$$

$$D = \frac{\varepsilon^2}{\delta^{2/3}}$$

$$E = 1.$$

In order to take into account a blade tip of nearly arbitrary shape a transformation of coordinates is made. This transformation has the general form :

$$\begin{cases} \xi = \xi(x,y) \\ \eta = \eta(y) \\ \zeta = \zeta(z) \end{cases}$$

In this coordinates system the blade leading and trailing edges are aligned with coordinated lines ξ = cst.

Details of the method, results and comparisons with experimental data can be found in [1 to 4]. Very good comparisons with experimental pressure measurements were obtained for a straight tip blade [3] ; however for a swept tip a too rapid disappearance of the shock wave in the second quadrant ($\Psi > 90°$) was predicted by the calculation [3] .

Equation (1) has been obtained in considering the transonic flow condition near the azimuth $\Psi = 90°$ for which the incident Mach number is maximum. A new approach has been studied in order to extend the domain of validity of the method for a larger azimuthal sector around $\Psi = 90°$. This approach is similar to the one used at RAE for the development of a quasi-steady calculation method for transonic flows on helicopter blade [5] . In coordinates along (s) and normal (n) to the local velocity vector the transonic small disturbances equation writes :

$$M_{\omega R}^2\,\varepsilon^2\,\phi_{tt} + 2\,M_{\omega R}^2\,\varepsilon\,\phi_{st}\sqrt{u_1^2+u_2^2} =$$

$$\phi_{ss}\left\{1 - M_{\omega R}^2\,(u_1^2+u_2^2) - M_{\omega R}^2\,(\gamma+1)\,\phi_s\sqrt{u_1^2+u_2^2}\right\}$$

$$+ \phi_{nn} + \phi_{33} + M_{\omega R}^2\,\varepsilon\,\phi_s\,\frac{1}{\sqrt{u_1^2+u_2^2}}\,(-u_2\,\mu\cos t + u_1\,\mu\sin t)$$

In a blade attached Cartesian coordinate system, this equation becomes :

$$M_{\omega R}^2 \varepsilon^2 \phi_{tt} + 2M_{\omega R}^2 \frac{\varepsilon}{\delta^{2/3}} u_1 \phi_{xt} - 2M_{\omega R}^2 \frac{\varepsilon^2}{\delta^{2/3}} u_2 \phi_{yt} =$$

$$\frac{1}{(u_1^2+u_2^2)} \left(u_1^2 \phi_{xx} + u_2^2 \varepsilon^2 \phi_{yy} - 2 u_1 u_2 \varepsilon \phi_{xy}\right) \left\{ \frac{1 - M_{\omega R}^2 (u_1^2+u_2^2)}{\delta^{2/3}} - M_{\omega R}^2 (\gamma+1)(u_1 \phi_x - \varepsilon u_2 \phi_y) \right\}$$

$$+ \frac{u_2^2}{(u_1^2+u_2^2)} \frac{\phi_{xx}}{\delta^{2/3}}$$

$$+ \frac{u_1^2}{(u_1^2+u_2^2)} \frac{\varepsilon^2}{\delta^{2/3}} \phi_{yy}$$

(1') $$+ \frac{2u_1 u_2}{(u_1^2+u_2^2)} \frac{\varepsilon}{\delta^{2/3}} \phi_{xy}$$

$$+ \phi_{zz}$$

$$+ \frac{\varepsilon}{\delta^{2/3}} M_{\omega R}^2 (\mu \sin t + u_2) \phi_x + \frac{\varepsilon^2 M_{\omega R}^2}{\delta^{2/3}} (u_1 + \mu \cos t) \phi_y$$

with $$\begin{cases} u_1 = y + \mu \cos t \\ u_2 = \varepsilon x + \mu \sin t \end{cases}$$

In this equation no hypothesis is made concerning the spanwise flow (u_2) relative to the chordwise one (u_1). For $\Psi \simeq 90°$ ($t = 0.$, $u_2 \simeq 0.$) and $M_{\omega R}^2 \varepsilon^2 \phi_{tt}$ negleted (low reduced frequency) the equation (1') is quite close to equation (1).

The ϕ_{yt} term and the modification of the transonic term (underlined) have been taken into account in a simplified way. In the coordinates system ξ, η, ζ linked to the shape of the blade only the derivative terms in ξ like $\frac{\partial \phi}{\partial \xi}$ and $\frac{\partial^2 \phi}{\partial \xi^2}$ have been kept for these two terms.

The surface tangency condition has been modified from : $\phi_z = (y + \mu \cos t) f'_x(x,y)$ to $\phi_z = (y + \mu \cos t) f'_x(x,y) - \mu \sin t \, \varepsilon f'_y(x,y)$, where $f(x, y)$ represents the equation of the upper, or lower surface of the blade.

These modifications have improved the results obtained for non-rectangular blade with a better prediction of the phase shift of the transonic flows on a 30° sweptback tip (Fig. 1) and a disappearance of the shock wave after $\Psi = 90°$ in good agreement with the experimental one. A better stability of the method has also been obtained and for all the calculations presented in this paper a time step of at least $\Delta\Psi = 1°$ has been used.

2.2 - *Lifting calculation* -

For lifting calculations the influence of the complex wake system has to be taken into account. As the calculations concern high advance-ratio flight configurations ($\mu > 0.3$), where the induced downwash is small, an angle-of-attack approach has been adopted.

The unsteady lifting calculations are performed on an isolated blade with an angle of attack prescribed along the blade for each azimuthal location by

$$\alpha(r/R, \Psi) = \theta_c + \theta_w (r/R - 0.7) + \alpha_1 + \alpha_2 + \alpha_3$$

The experimental values are used for the rotor shaft angle, the collective pitch angle, the blade twist angle and the flapping angle. The induced incidence (α_3) has been calculated using the simple DREES downwash model [6]. More details concerning this angle-of-attack approach and some results can be found in [7].

For the boundary condition on the wake, the spanwise velocity component is now taken into account. This gives an oblique wake for the azimuts different of 90°.

3 - NON-LIFTING UNSTEADY CALCULATION RESULTS -

Different tip shapes have been studied (Fig. 2) :

- rectangular,
- swept back tip of 30° between .9R and R (F30)
- swept forward tip of 30° between .9R and R (F-30),
- progressive swept tip with taper (PF2),
- rectangular with an anhedral tip of 10° between .9R to R.

The calculations results presented Fig. 3 to 11 correspond to the following conditions : advance ratio $\mu = 0.5$, $M_{\omega R} = .64$, blade with a profile of constant thickness $\delta = 11\%$., low aspect ratio = 7.

The supersonic flows occuring on the blades are characterized by the evolution of the maximum local Mach number and the one of the extent of supercritical flows.

3.1 - Comparison between rectangular, F30, F-30 blade tips : (Figs. 3-4)

The evolutions of the maximum local Mach number versus span location are compared for the rectangular blade, F30 and F-30 at different azimuths (Fig. 3).

Compared to the rectangular blade :

- at $\Psi = 60°$, the intensity of the transonic flows decreases for the sweptback tip on the last 15% of the blade (between .85R and R) ; on the swept forward tip an higher Mach number is observed at the beginning of the swept tip (.9R),
- at $\Psi = 90°$ a slight expansion can be noticed on the constant sweptback tip.
- after $\Psi = 90°$ this expansion on F30 increases and spreads along the blade.

The evolution of the maximum local Mach number with the azimuthal location and the one of the extent of supercritical flows show a phase shift of the supersonic flows with sweep :

- on the sweptback tip, the supercritical flows appear later in azimuth (compared to the straight tip) with a decrease of their intensity before $\Psi = 90°$, and disappear later after 90° with an increasing expansion at the tip,

- on the swept forward tip an opposite effect can be observed ; the supercritical flows appear sooner in azimuth before 90° and disappear sooner after 90°.

3.2 - *Comparison between rectangular, F30, PF2 blade tips* - (Figs. 5-6)

The leading edge line of the PF2 tip has a parabolic shape between .95R and R and the sweep angle of the leading edge is 80° at the tip. A more precise definition of this PF2 tip defined at ONERA can be found in [9] . The intensity of the transonic flows is smaller on this PF2 tip compared to the straight one for almost all the advancing blade side. In particular the expansion seen on F30 is strongly reduced and at $\Psi = 90°$ the maximum local Mach numbers are the smallest for the last 20% of the blade span for this PF2 tip. However for $130° < \Psi$ the transonic flows are slightly stronger on the PF2 tip than on the straight tip.

The isomach-lines at $\Psi = 60$, 90 and 120° (Figs. 7-8-9) give an overall view of the flows on the four different blade tips. The intensity of the transonic flows is strongly reduced on the PF2 tip where a weak shock becomes visible only at $\Psi = 120°$.

3.3 - *Unsteady effect of an anhedral tip* - (Figs. 10-11)

The blade considered is a rectangular one with an anhedral tip of 10° between .9R and R.

The pressure distributions at the radial station .95R (Fig. 10) and the lift coefficient azimuthal evolutions at .91R and .95R show that the effects of the anhedral tip are :

- to give a positive lift before 90° and a negative lift after 90° as it was expected,
- to increase the transonic flows on the upper surface before 90° and to decrease them after 90°.

This effect can be combined with planform shapes one to reduce the intensity of the transonic flows on the upper surface of a blade for forward flight at high advance ratio.

These "non-lifting" calculations show that an optimized blade tip shape for the whole advancing blade side is not easy to define. A constant swept tip weakens the shock intensity around the azimuth $\Psi = 90°$. As the incident Mach number is maximum for this azimuth such effect should improve the aerodynamic performances of a rotor by decreasing the drag and have favorable effect on the acoustic characteristics by lessening what acousticians call delocalization. However a part of this improvement can be lost by stronger shock in another azimuthal sector, for example in the second quadrant for a constant swepback tip. One possible solution is to take a progressive swept tip like the PF2 one with large sweep angle at the tip in order to extend the azimuthal sector where the shocks are weakened. An other possibility could be to combine sweep and anhedral geometry.

Experimental results obtained with a lifting model rotor [8] as well as flight test results [9] have confirmed the improvements expected with new tip shapes like the PF2 one. The lifting calculations presented below show that it becomes possible to predict the unsteady flows on such tip shapes for the advancing blade side.

4 - LIFTING UNSTEADY CALCULATION RESULTS -

The method described in [7] and 2.2 has been used to perform unsteady lifting calculations for three blade tips :

- rectangular one as a reference,
- an RAE swept tip designed by the Royal Aircraft Establisment [8] ,
- a FL5 swept tip designed by ONERA.

The results are compared with experimental ones obtained on a model rotor equiped with absolute pressure transducers at radial stations .85R, .9R and .95R. The tests were performed in S2 Chalais Meudon wind-tunnel with a twisted 3-bladed rotor.

4.1 - Comparisons between experimental and calculated results for the straight tip -

Some results concerning the configurations $\frac{C_T}{\sigma} = 0.05$, Vo = 76 m/s and $\frac{C_T}{\sigma} = 0.0665$, Vo = 81 m/s have already been published in [7] .

Results obtained for a more loaded case ($\frac{C_T}{\sigma} = 0.075$) at higher forward speed (Vo = 91 m/s) are presented on figures 12 and 13. The evolution of the pressure distributions with azimuth (Fig. 12) and the pressure coefficients at different chordwise locations of the span section .9R are well predicted (Fig. 13). In particular the development of a strong shock on the upper surface of the blade between $\Psi = 80°$ and $\Psi = 160°$.

The comparisons presented on figures 14 to 16 show that the calculation is able to predict the evolution of the transonic flows on the blade for conditions of loads and forward speeds more and more severe. A shock wave is still visible at the azimuth $\Psi = 150°$ for the configuration $\frac{C_T}{\sigma} = 0.075$, Vo = 91 m/s whereas the flow is only slightly transonic for the case $\frac{C_T}{\sigma} = 0.05$, Vo = 76 m/s.

In general the calculation gives a shock wave with a slightly stronger intensity and located more downstream than in the experiment. This can be due to the simple inflow model used but more likely to the lack of any viscous effect in the calculations. This has been shown in 2D unsteady calculations [10] and the results obtained by 3D quasi- steady calculation with and without boundary layer corrections show the same tendancy (Fig. 17).

4.2 - Comparisons between experimental and calculated results for the RAE tip -

The RAE progressive swept tip designed by the Royal Aircraft Establishment (Fig. 18)has a leading edge sweep angle of the order of 75° at the tip.

The results presented on figure 19 concern the configuration $\frac{C_T}{\sigma} = .0665$, Vo $\simeq$ 82 m/s. The experimental and calculated evolutions with azimuth of

the maximum local Mach number and of the extent of supercritical flow for the RAE and the straight tips illustrate the influence of a progressive sweptback tip :

. a clear decrease of the intensity of the transonic flows around $\Psi = 90°$,
. a delay in the appearance of transonic flows on the swept tip with a tendancy to maintain supercritical flows longer in the second quadrant.

The upper-surface pressure distributions at $\Psi = 90°$ (Fig. 20) show that the effects of the progressive sweptback tip increase with forward speed. On the swept tip the shocks strength is still relatively weak at the forward speed of 90 m/s. More experimental results concerning this RAE tip can be found in [8] .

4.3 - *Comparisons between experimental and calculated results for the FL5 tip* -

The FL5 progressive swept tip design by ONERA (Fig. 18) has a linear evolution of the leading edge sweep angle between R-1.05 c and R-0.52c and an another one between R-0.52c and R with a value of 72.5° at the tip.

Pressure distributions for sections .9R (Fig. 21) and .95R (Fig. 22) at different azimuths show good agreement between experimental results and calculated ones. The evolutions of the pressure coefficient at different chordwise locations of the section .95R are relatively smooth without sharp discontinuities that the motion of a strong shock would give. This was not the case for the straight tip (Fig. 13) where the result of the backward and forward motions of a strong shock wave are quite visible. However the isomach lines on the upper surface presented Fig. 24 show supercritical flow evidence up to the span section .5R at $\Psi = 120°$ and 150°.

In spite of transonic flows of slightly higher intensity on RAE and FL5 tips (Fig. 25) after $\Psi = 140$ or 150°, the clear decrease of their intensity for $\Psi < 130°$ is certainly the main reason of the improvement in the performances obtained with the model rotor equiped with the swept tips compared to the ones of the same rotor equiped with rectangular blades. At high speed and high lift an improvement of 7-8% for the power required by the rotor has been obtained with the FL5 tip (Fig. 26).

These calculated results obtained for the rectangular, RAE and FL5 blades are very encouraging and give a certain confidence in using such a method as an help to design efficient tip shapes for fast forward flight. However improvements of the method should be probably obtained with the use of a more sophisticated inflow model like the vortex point method developed at ONERA [11] . All the results presented concern very stiff blade and the influence of some deformations is going to be studied for comparisons with flight test results.

5 - *CONCLUSION* -

An unsteady transonic small perturbations method has been used to predict the flows on an helicopter blade in the advancing blade side where unsteady transonic flows occur. Non lifting and lifting calculations have been performed for different tip shapes.

The non lifting unsteady calculations concern :

- a rectangular blade,
- a swept back tip,
- a swept forward tip,
- a progressive swept tip with taper,
- a rectangular tip with an anhedral geometry.

They show that an optimized blade tip shape for the whole advancing blade side is not easy to define. A constant swept tip weakens the shock intensity around the azimuth $\psi = 90°$ but give a stronger shock in an other azimuthal sector. A progressive swept tip with large sweep angle at the tip extends the azimuthal sector (around 90°) where the shocks are weakened. Positive results could certainly be obtained by combining sweep and anhedral.

The lifting calculations concern high advance ratio configurations ($\mu > 0.3$). Three blade tips were considered : a rectangular and two evolutive swept tips. The resulting computations compare well with experimental results obtained on a model rotor equiped with absolute pressure transducers. The experimental and calculated results indicate clearly that the improvement of the performances, obtained with the model rotor equiped with the swept tips compared to the ones of the same rotor equiped with rectangular blades, is mainly due to the decrease of the transonic flow intensity observed on the swept tips. All these results are very encouraging and give a certain confidence in the use of such a method as an help to design efficient tip shapes for fast forward flight.

Improvements of the method should be obtained with the use of a more sophisticated inflow model than the J. DREES formulation ; in particular for lower advance ratios for which the downwash level is larger. Development of unsteady full potential or Euler equations codes would also increase the domain of validity of such method.

REFERENCES -

1 J.J. CHATTOT
Calculation of three-dimensional unsteady transonic flow past helicopter blades
NASA TP 1721, AVRADCOM TR 80-A-2 (AM), 1980

2 F.W. CARADONNA, M.P. ISOM
Numerical calculation of unsteady transonic flow over helicopter rotor blades.
AIAA Journal, Vol. n° 14 n° 4 (April 1976)

3 J.J. CHATTOT, J.J. PHILIPPE
Pressure distribution computation on a non-lifting symetrical helicopter blade in forward flight.
La Recherche Aérospatiale (English version), n° 1980-5

4 J.J. PHILIPPE, A. VUILLET
Aerodynamic design of advanced rotors with new tip shape.
39th Forum "American Helicopter Society"
Saint-Louis (Missouri) 9-11 May 1983

5 J. GRANT
Calculation of the supercritical pressure distributions on blade tips of arbitrary shape over a range of advancing blade azimuth angles.
4th European Rotorcraft and Powered Lift Aircraft Forum, Stresa (Italia), September 1978.

6 J.M. DREES
A Theory of Airflow Through Rotors and its Application to some Helicopter Problems .
Journal of the Helicopter Association of Great Britain, vol. 2, 1949

7 F.X. CARADONNA, A. DESOPPER, C. TUNG
Finite Difference Modeling of Rotor Flows including Wake Effects.
8th European Rotorcraft Forum - Aix en Provence (1982)
TP ONERA n° 1982-114

8 P. WILBY, J.J. PHILIPPE
An investigation of the aerodynamics of an RAE swept helicopter blade tip using a rotor model.
8th European Rotorcraft - Aix en Provence (1982)
T.P. ONERA 1982-76

9 F. GUILLET, J.J. PHILIPPPE
Flight tests of a sweptback parabolic tip on a Dauphin 365 N
10th European Rotorcraft Forum - The Hague (1984)

10 A. DESOPPER, R. GRENON
Couplage fluide parfait-fluide visqueux en écoulement instationnaire bidimensionnel incompressible et transsonique.
Computation of Viscous-Inviscid Interactions.
AGARD-CP-291, 1980

11 B. CANTALOUBE, S. HUBERSON
A new approach using vortex point method for prediction of rotor performance in hover and forward flight
9th European Rotorcraft Forum-Stresa (1983)

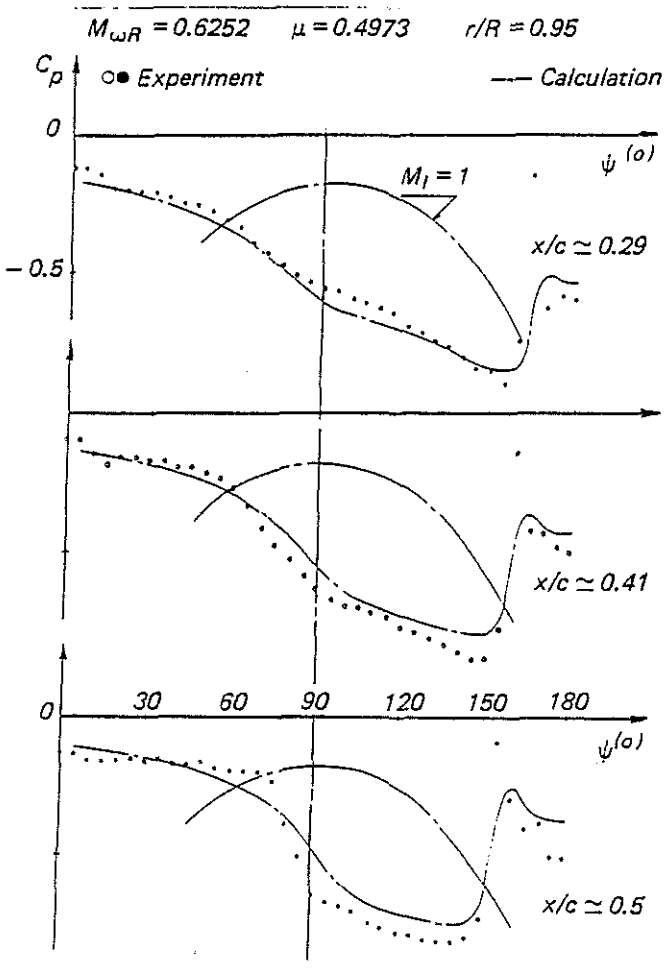

Fig. 1 – 30° swept back tip

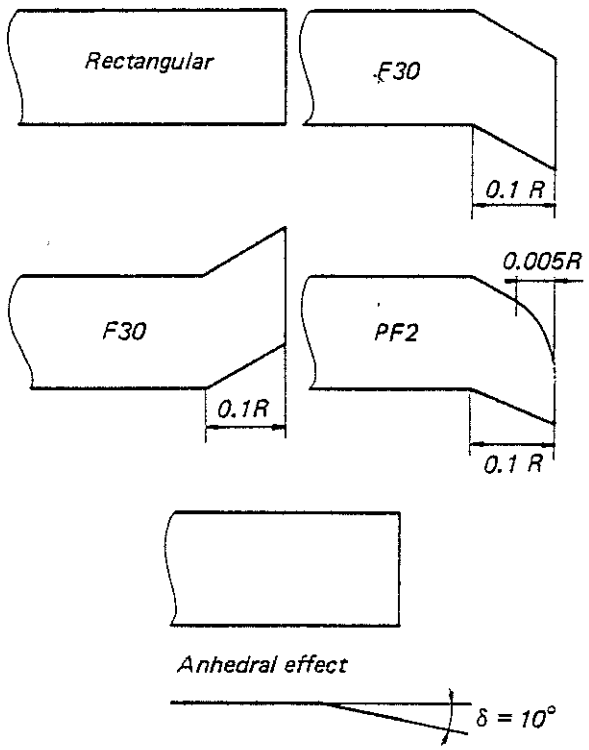

Fig.2– Study of different tip shapes .
Non lifting unsteady calculations

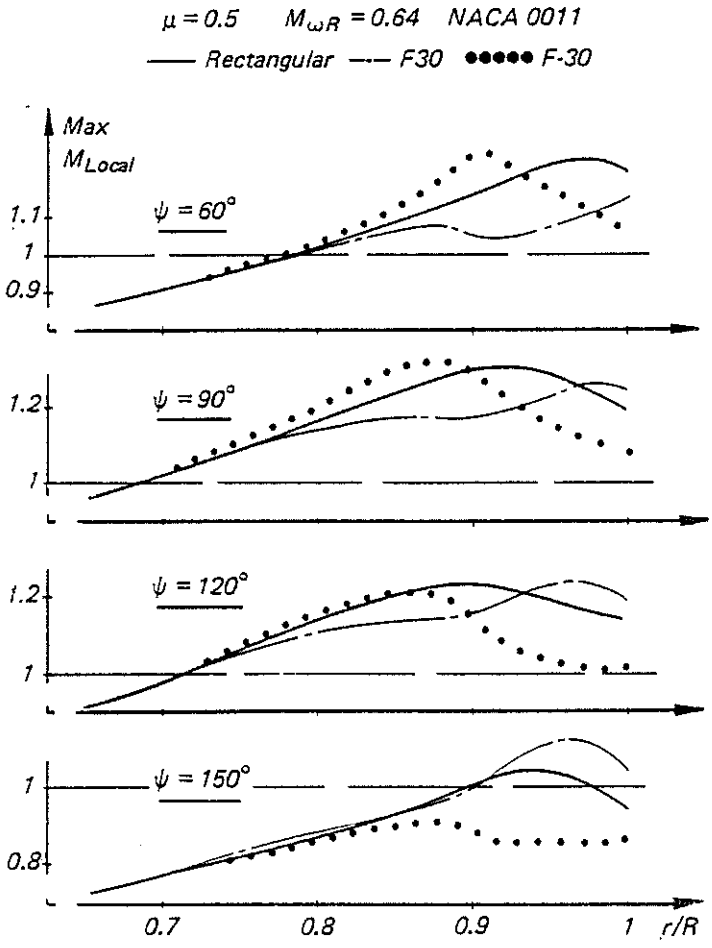

Fig.3– Study of different tip shapes .
Non lifting unsteady calculations

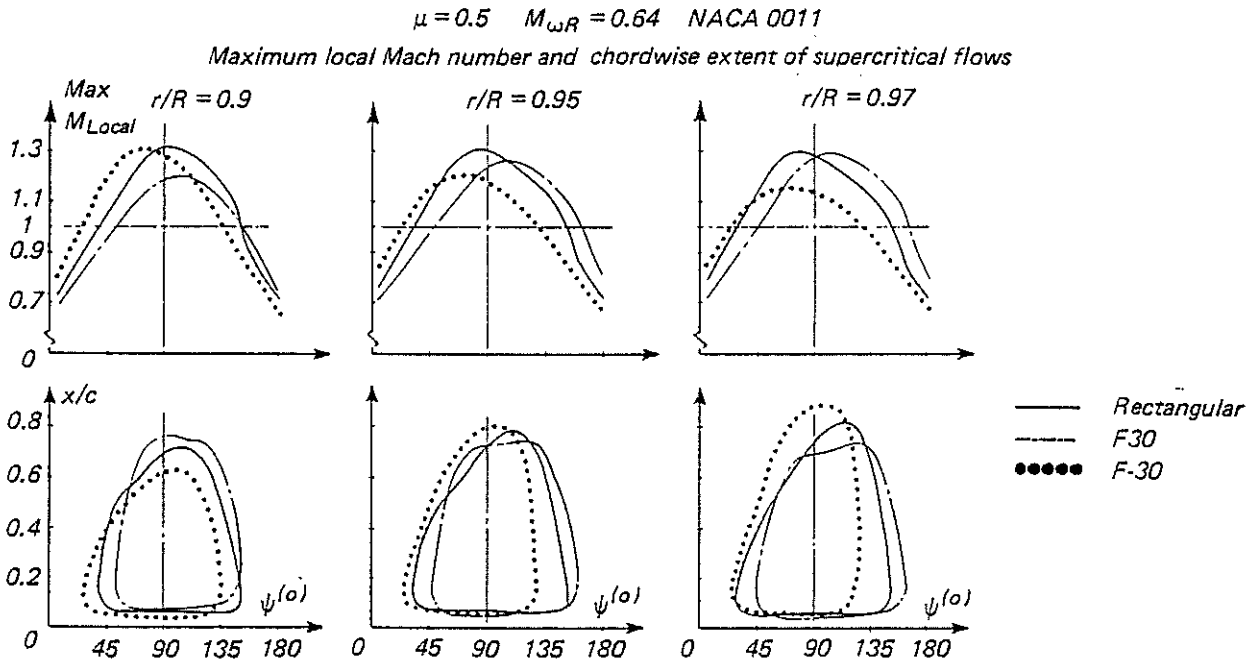

Fig.4– Study of different tip shapes. Non lifting unsteady calculations

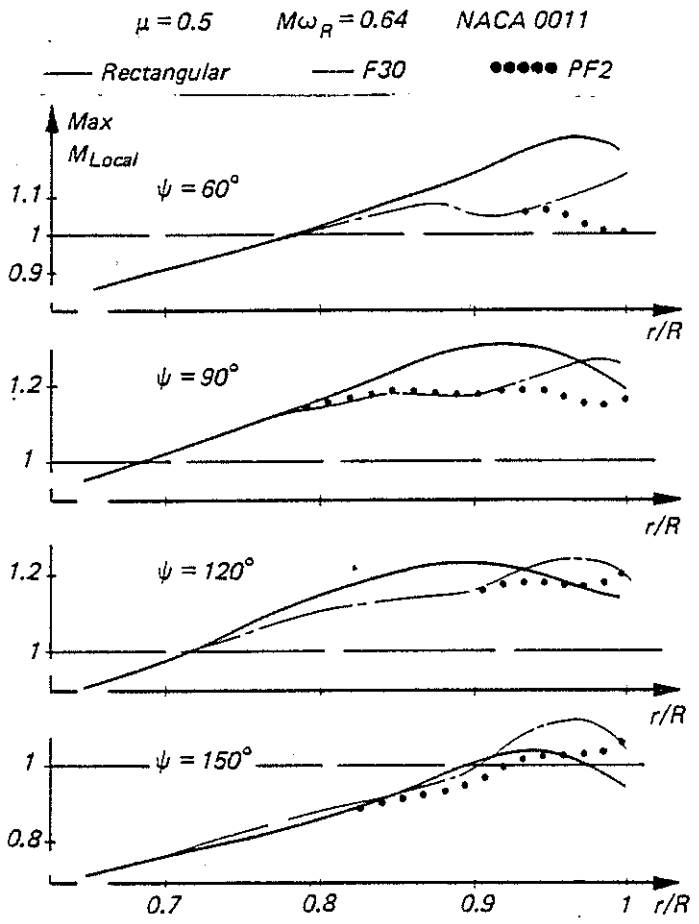

Fig.5— Study of different tip shapes . Non lifting unsteady calculations

Maximum local Mach number and chordwise extent of supercritical flows

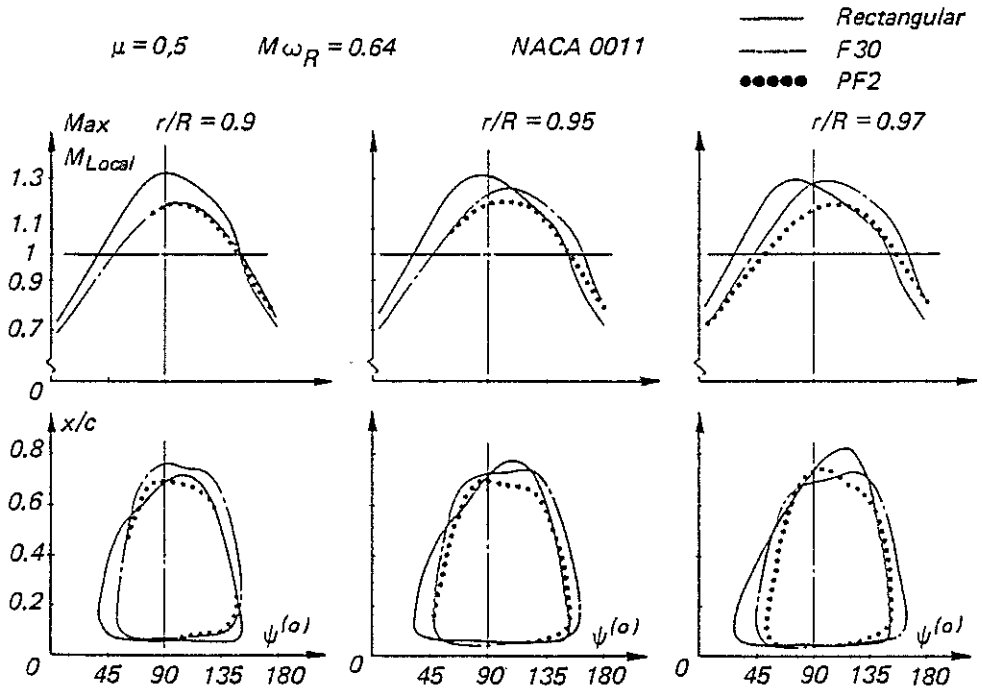

Fig.6— Study of different tip shapes . Non lifting unsteady calculations

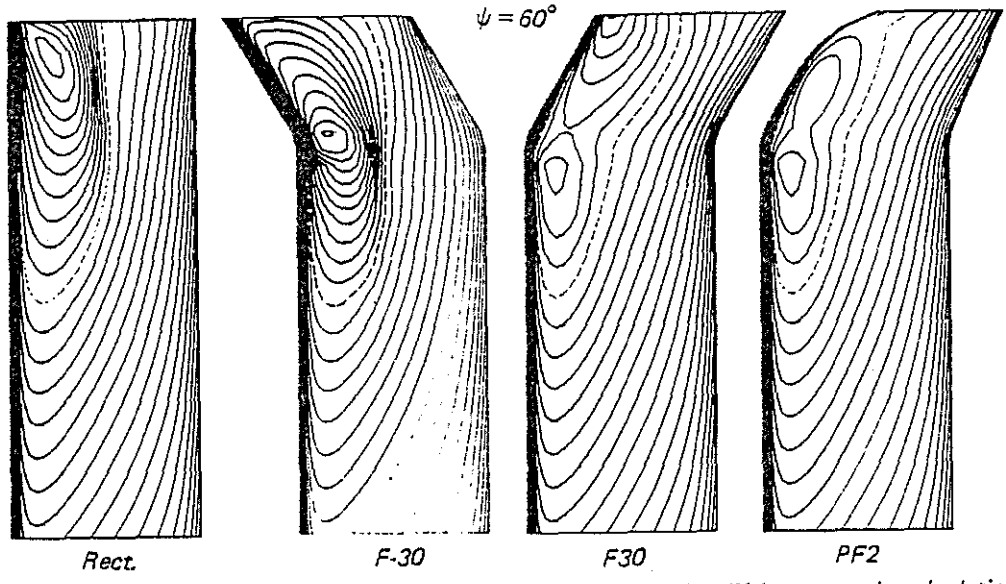

Fig.7— Study of different tip shapes. Non lifting unsteady calculations

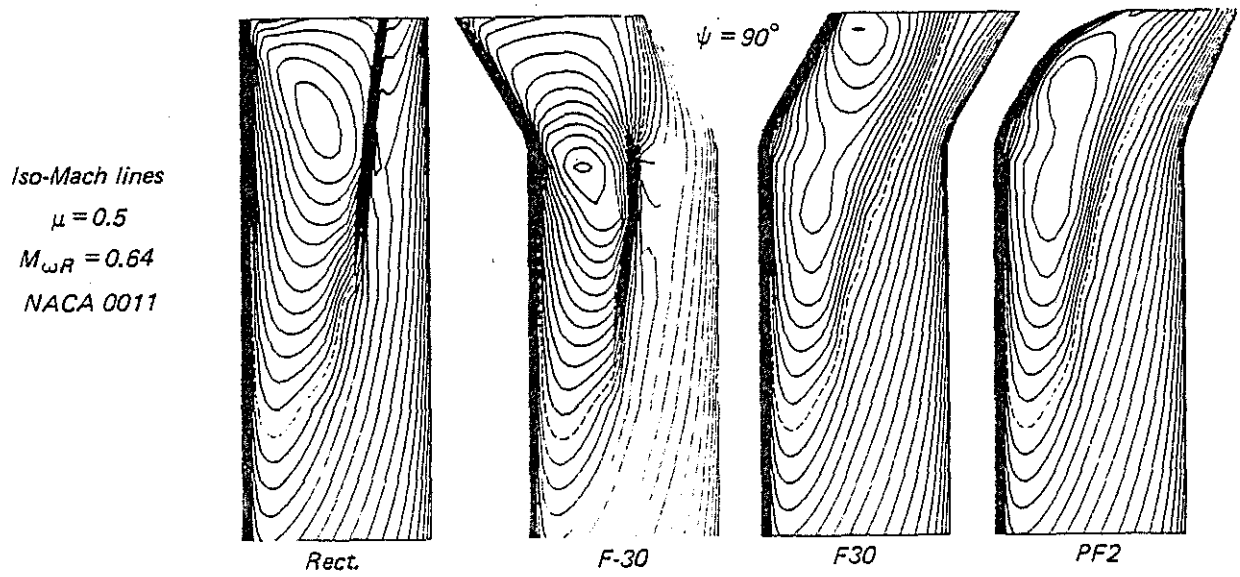

Fig.8— Study of different tip shapes. Non lifting unsteady calculations

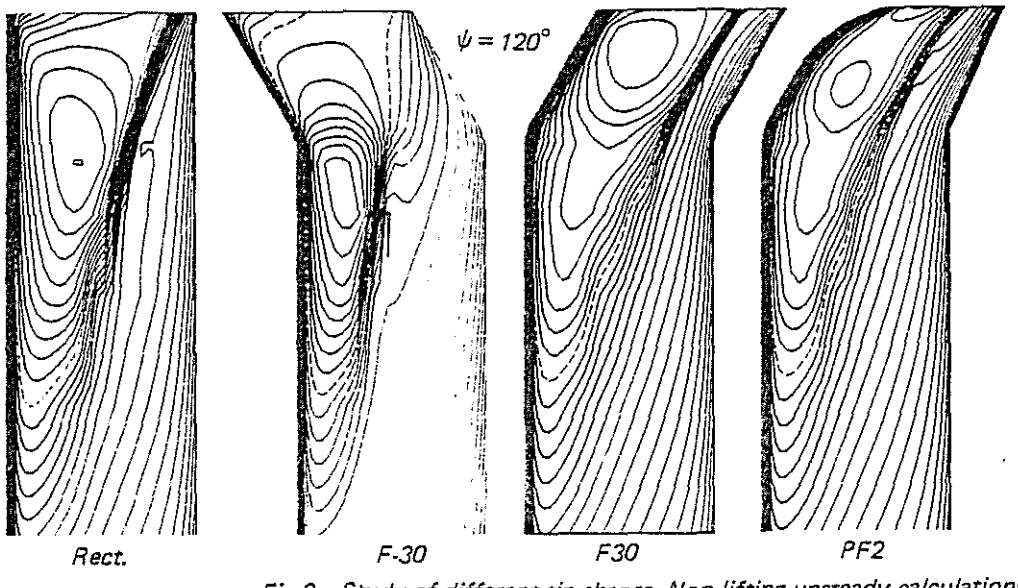

Fig.9— Study of different tip shapes. Non lifting unsteady calculations

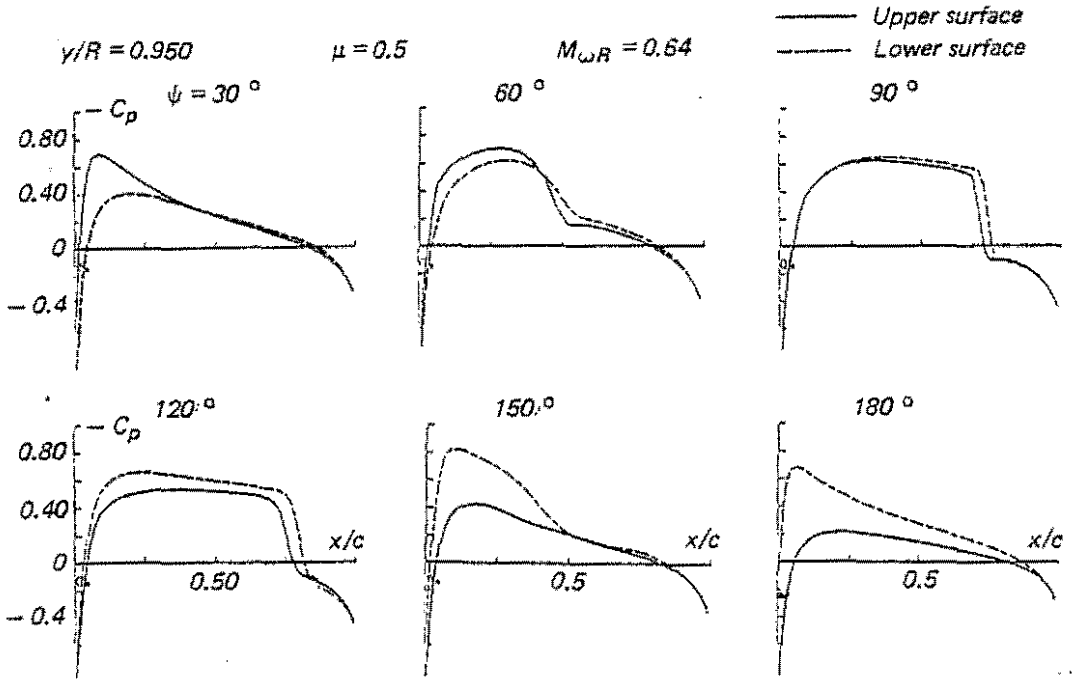

Fig.10– Unsteady calculations. Rectangular blade with anhedral tip

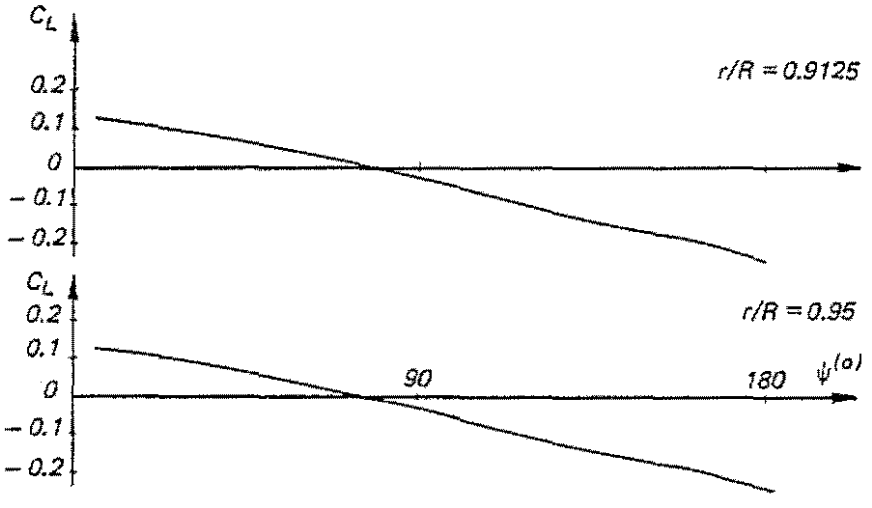

Fig.11– Unsteady calculations. Rectangular blade with anhedral tip

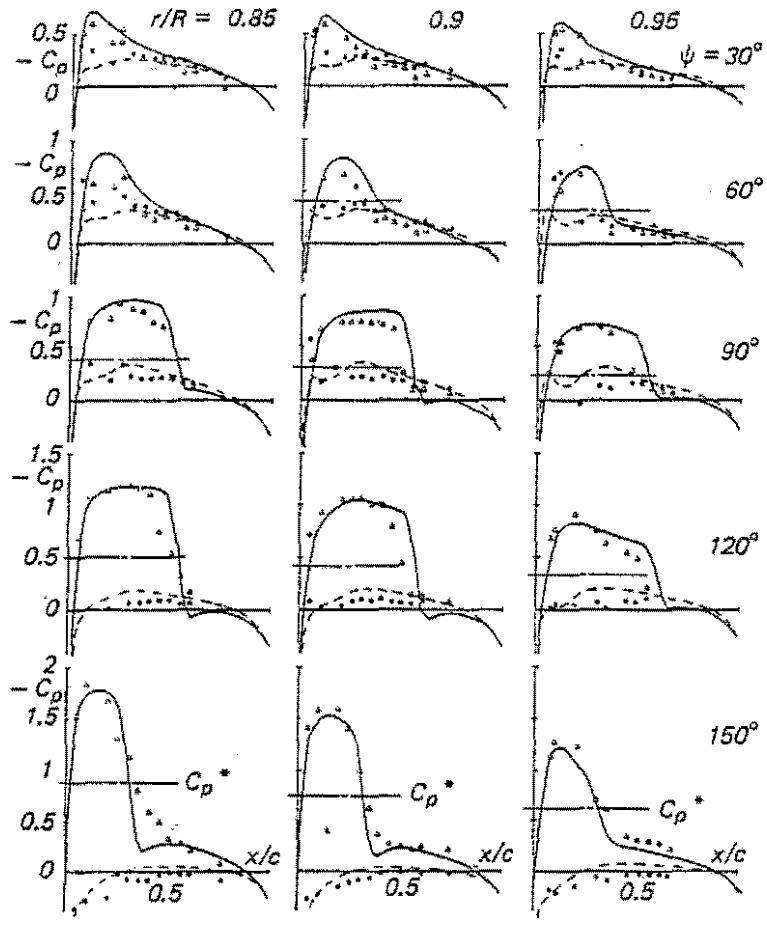

Fig.12— Lifting unsteady calculation. Rectangular blade

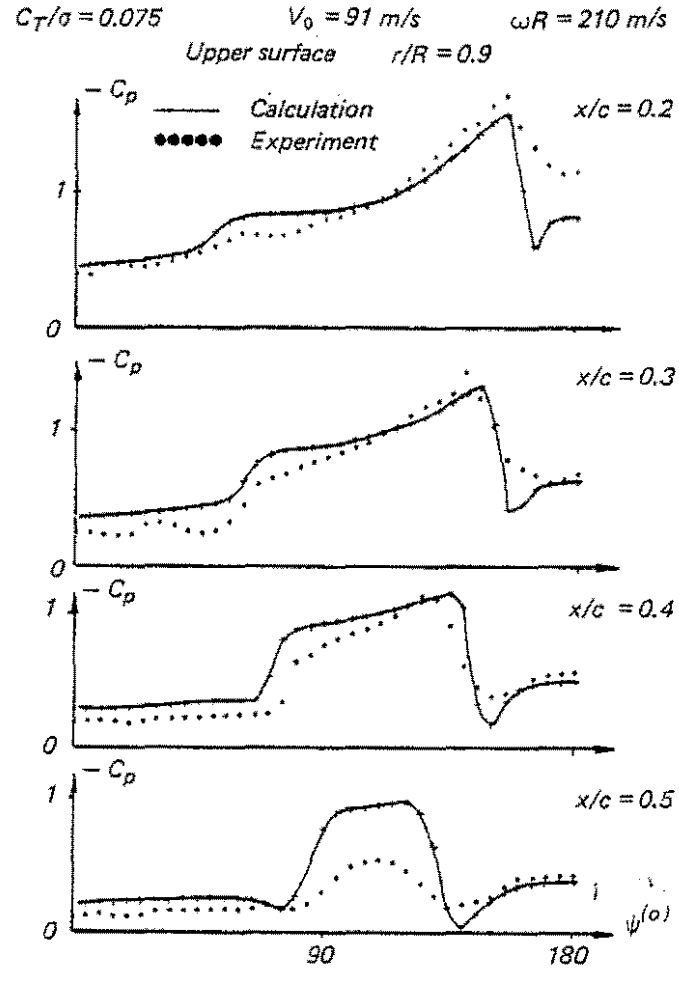

Fig.13— Lifting unsteady calculation . Rectangular blade

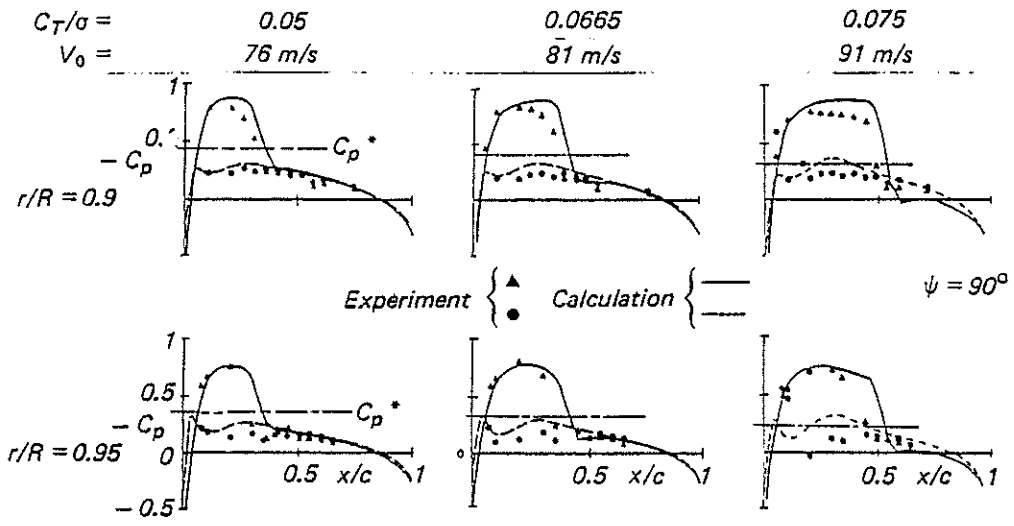

Fig.14— Lifting unsteady calculation. Rectangular blade

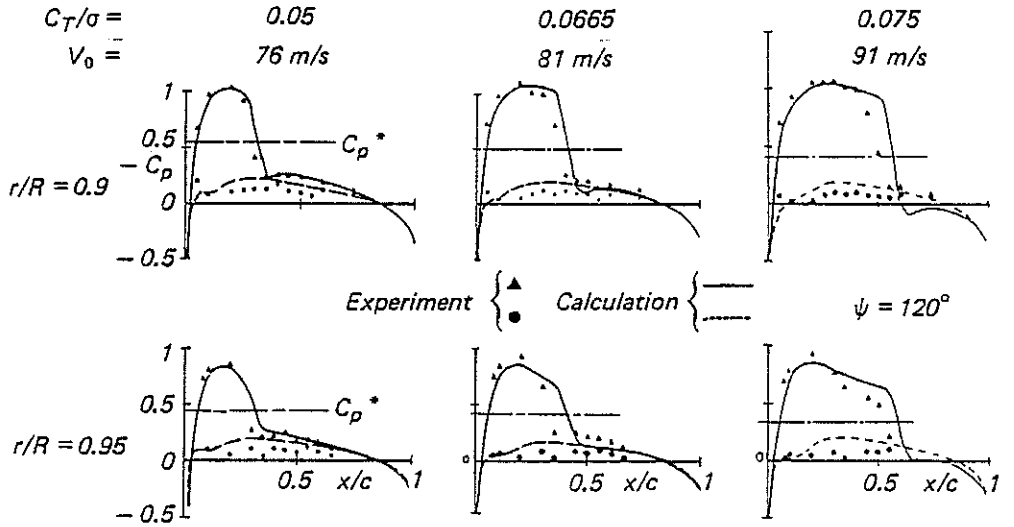

Fig.15— Lifting unsteady calculation. Rectangular blade

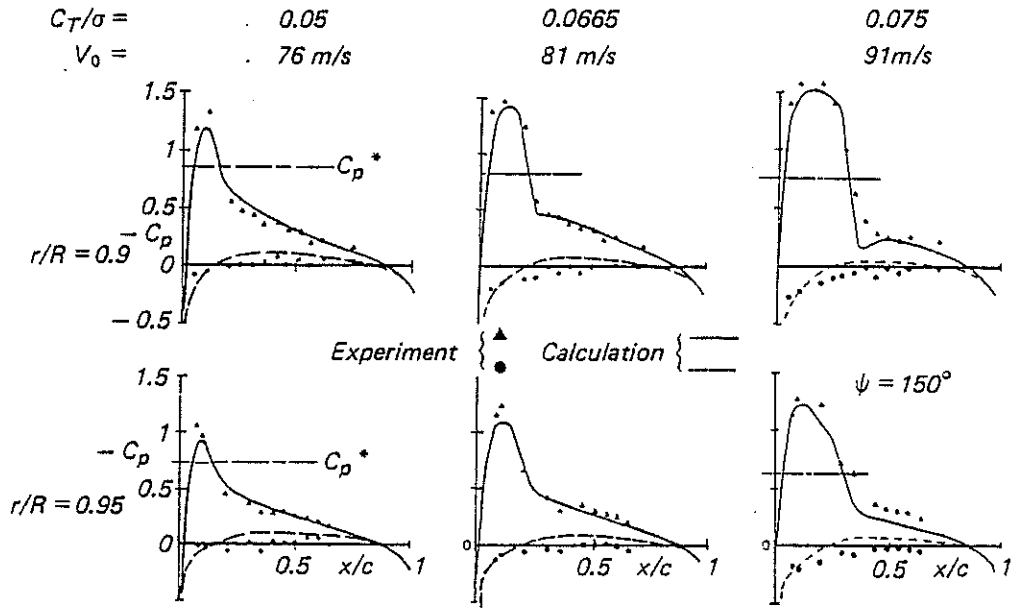

Fig.16 — Lifting unsteady calculation. Rectangular blade

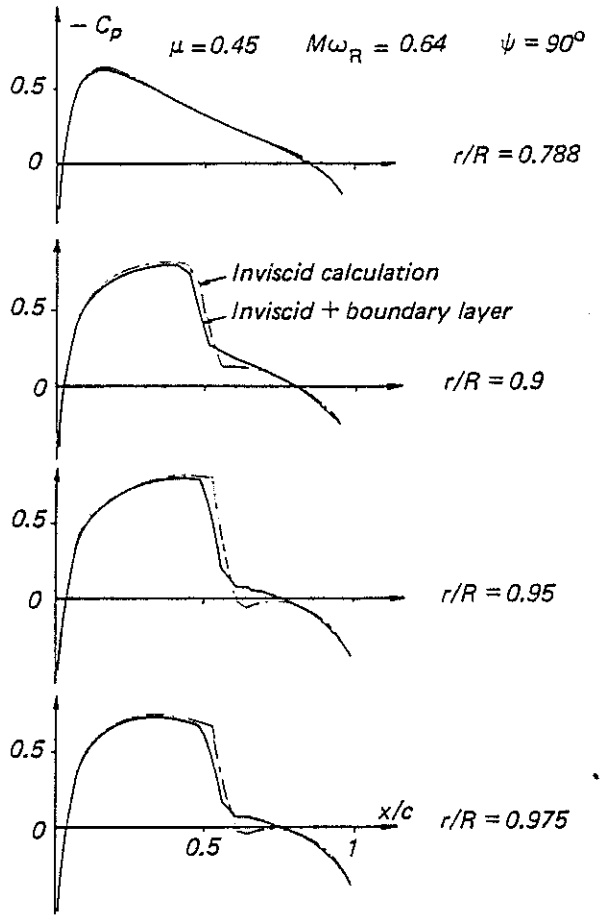

Fig. 17 — Quasi steady calculations . Influence of viscous effect

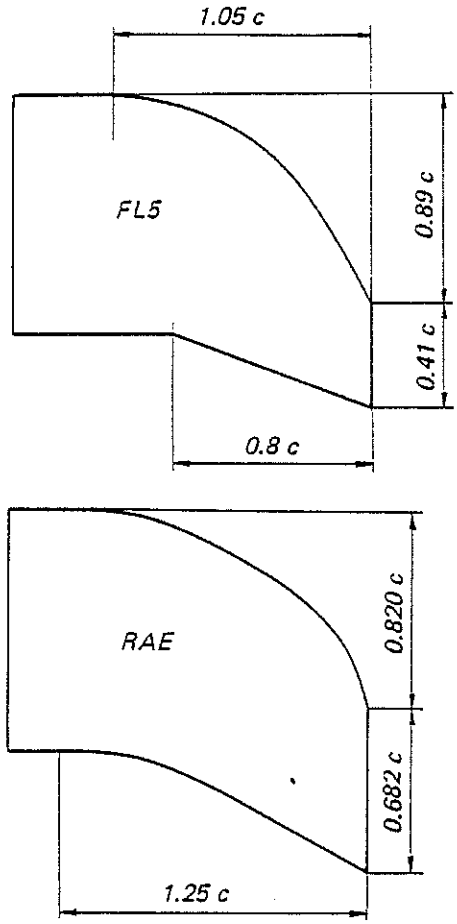

Fig.18— FL5 and RAE tips blade

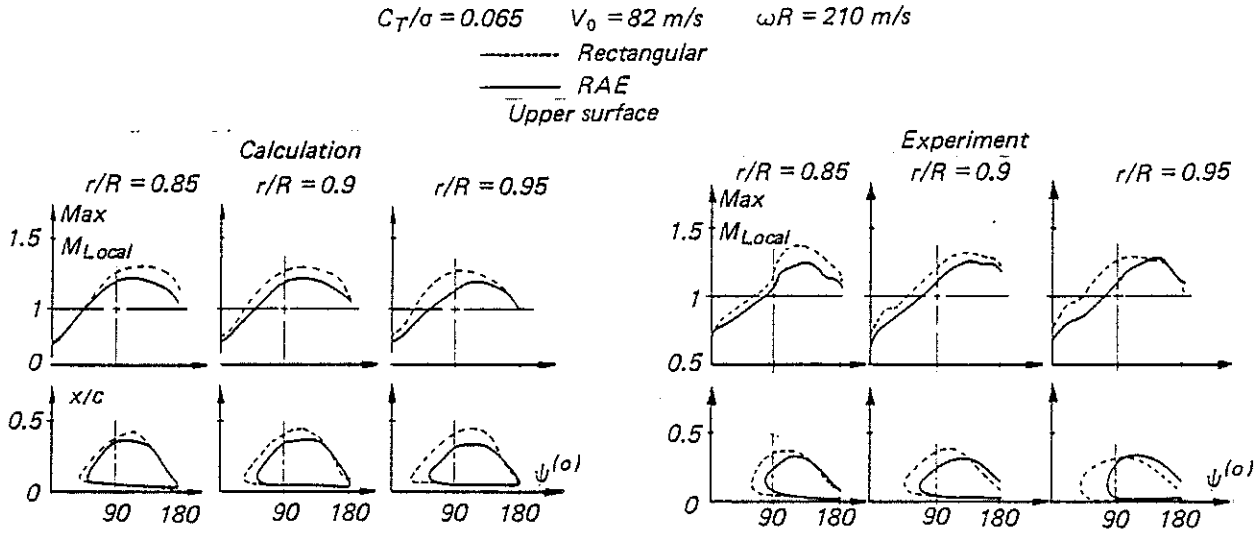

Fig.19— Lifting unsteady calculations. Rectangular and RAE blades

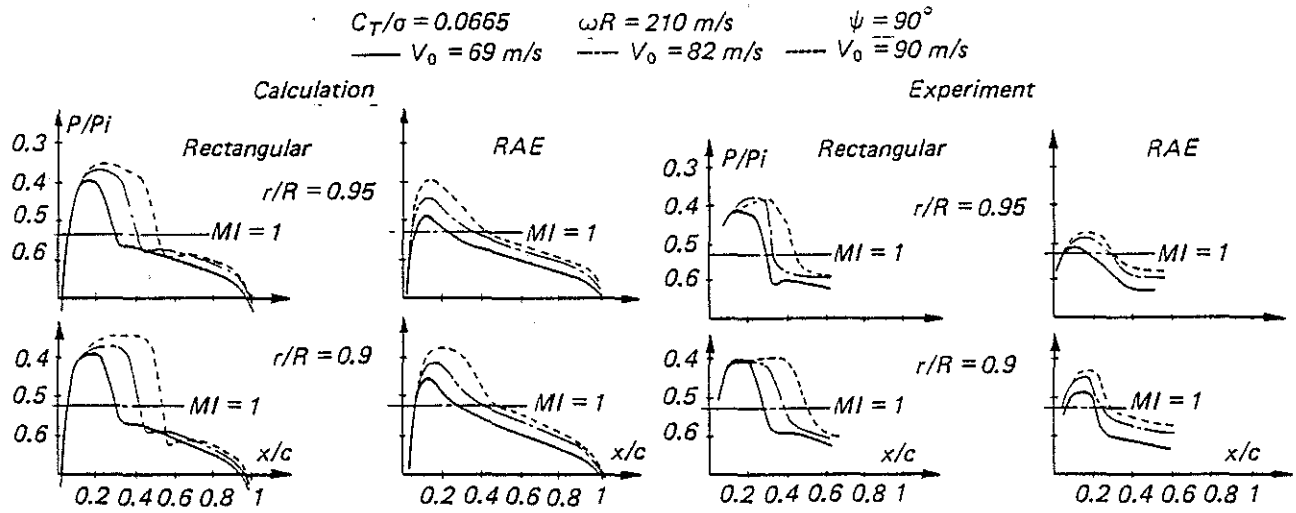

Fig.20– Lifting unsteady calculations. Rectangular and RAE blades

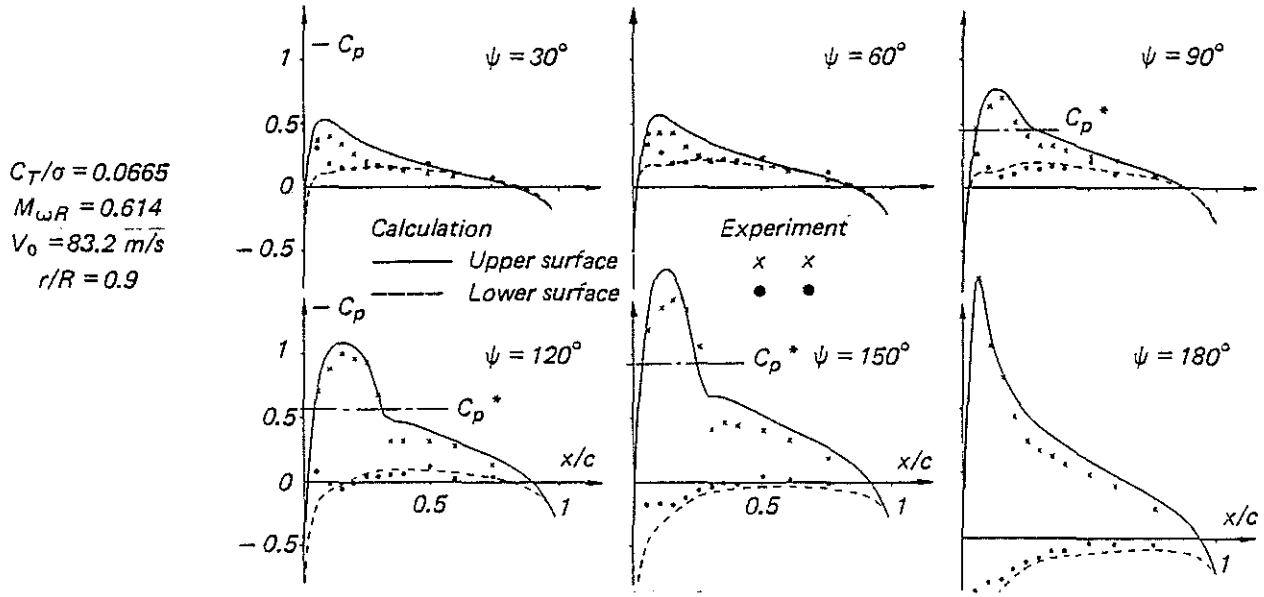

Fig.21– Lifting unsteady calculation . FL5 blade

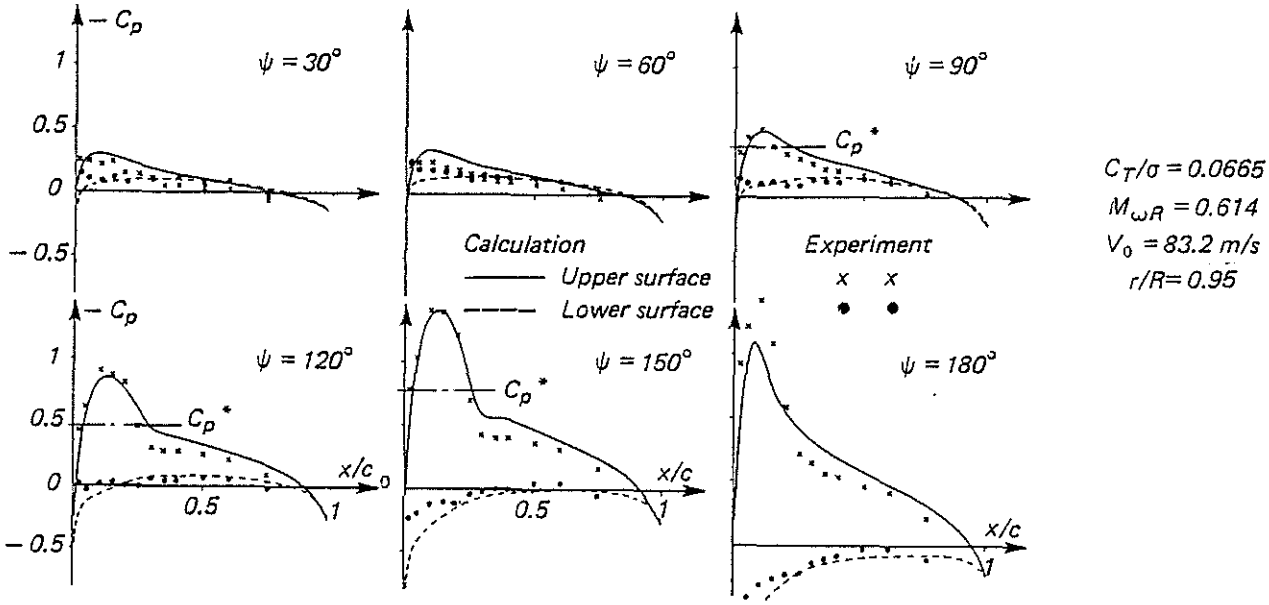

Fig.22– Lifting unsteady calculation. FL5 blade

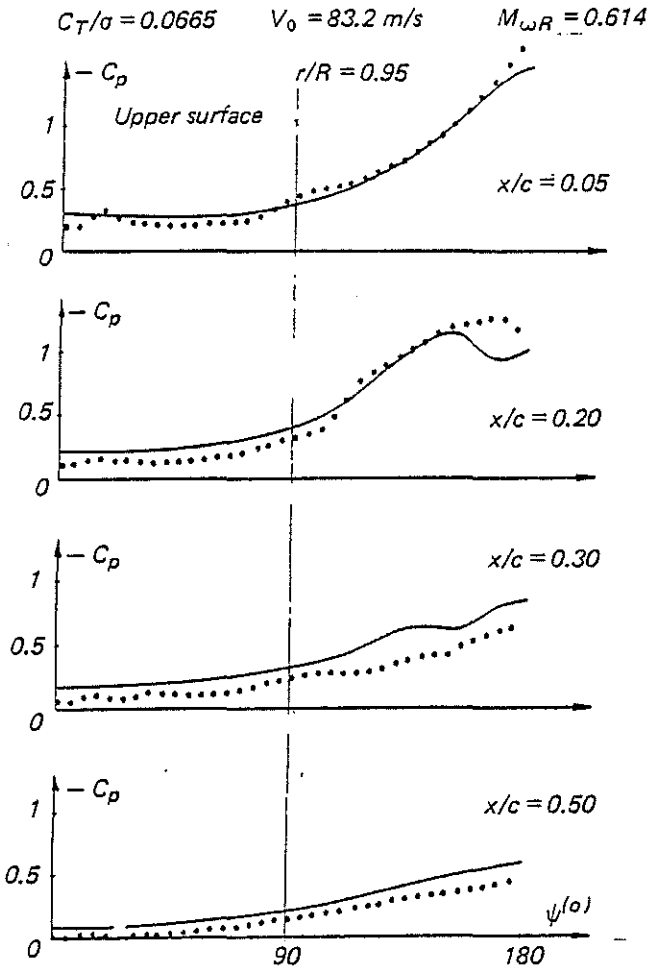

Fig.23– Lifting unsteady calculation . FL5 blade

—— *Calculation*
●●●● *Experiment*

Iso-Mach lines (upper surface)

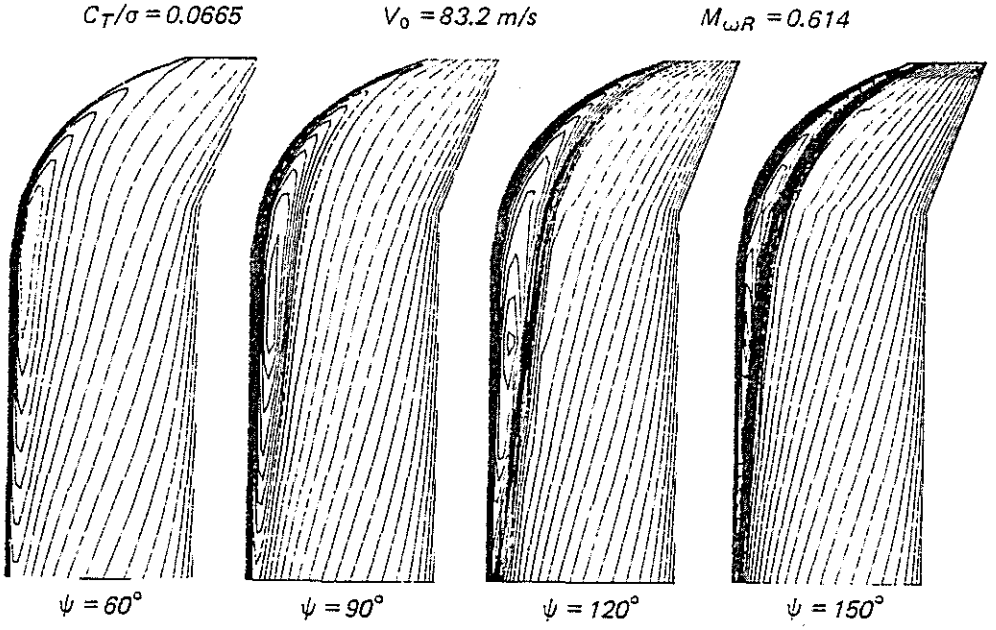

Fig.24– Lifting unsteady calculation.FL5 blade

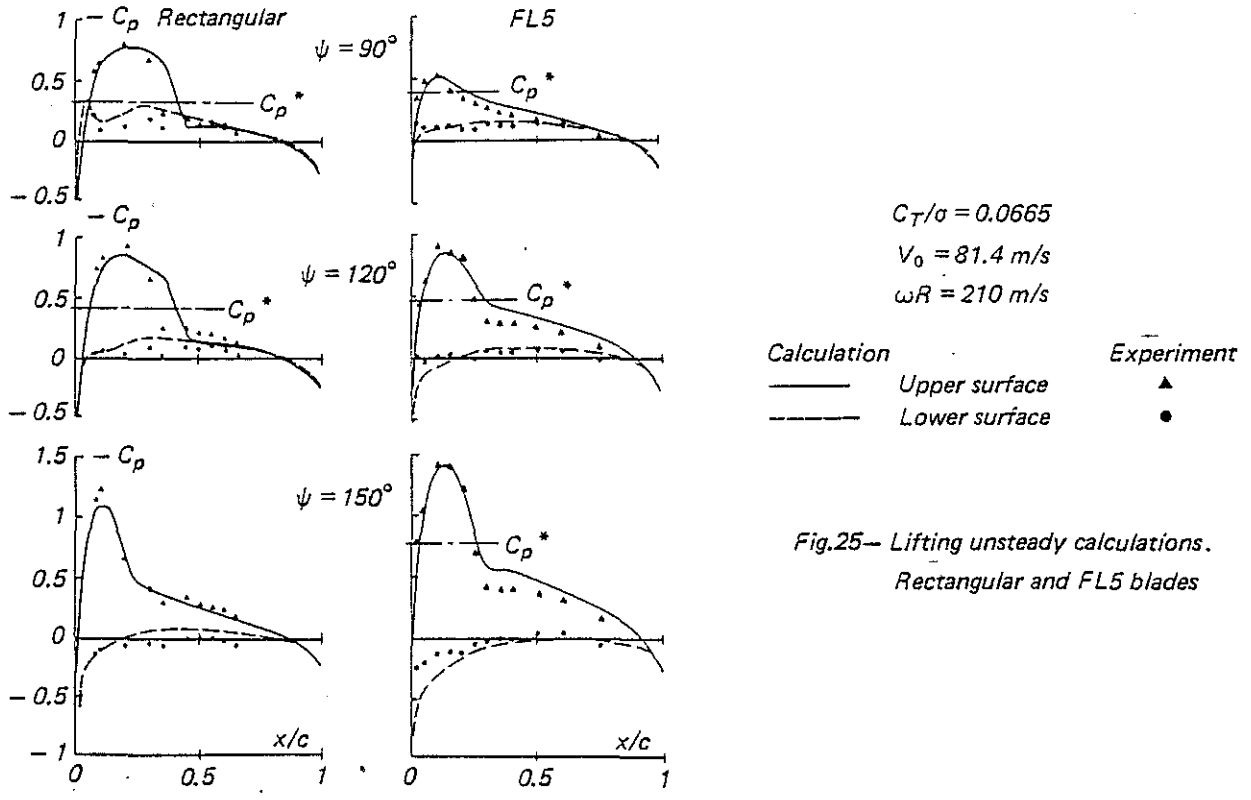

Fig.25– Lifting unsteady calculations. Rectangular and FL5 blades

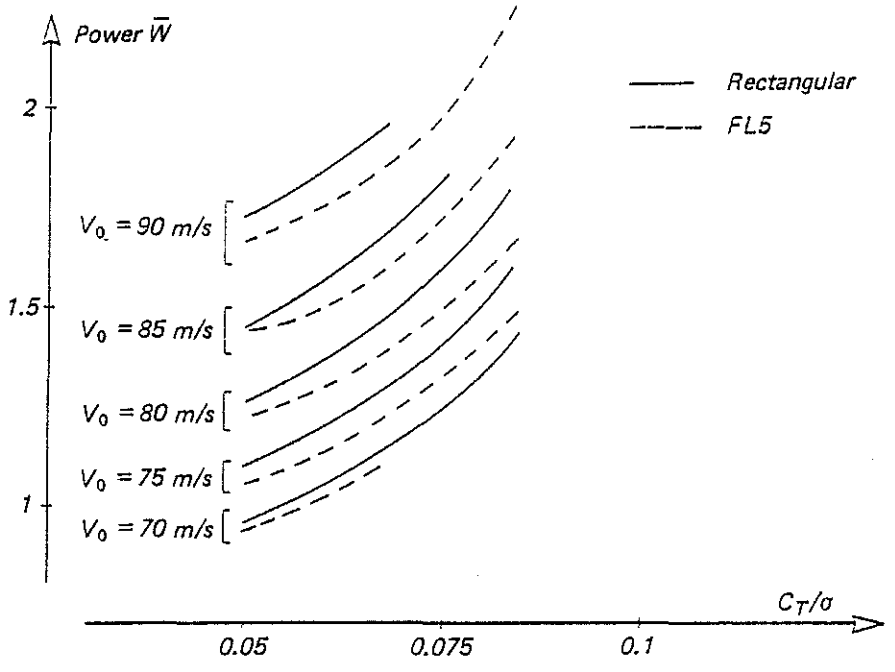

Fig.26– Power required by a rotor